Acta Neuropathologica Communications

RESEARCH

Open Access

Crucial role of Aquaporin-4 extended isoform in brain water Homeostasis and Amyloid-β clearance: implications for Edema and neurodegenerative diseases

Pasqua Abbrescia[1†], Gianluca Signorile[1†], Onofrio Valente[1], Claudia Palazzo[1], Antonio Cibelli[2], Grazia Paola Nicchia[2] and Antonio Frigeri[1*]

Abstract

The water channel aquaporin-4 (AQP4) is crucial for water balance in the mammalian brain. AQP4 has two main canonical isoforms, M23, which forms supramolecular structures called Orthogonal Arrays of Particles (OAP) and M1, which does not, along with two extended isoforms (M23ex and M1ex). This study examines these isoforms' roles, particularly AQP4ex, which influences water channel activity and localization at the blood-brain barrier. Using mice lacking both AQP4ex isoforms (AQP4ex-KO) and lacking both AQP4M23 isoforms (OAP-null) mice, we explored brain water dynamics under osmotic stress induced by an acute water intoxication (AWI) model. AQP4ex-KO mice had lower basal brain water content than WT and OAP-null mice. During AWI, brain water content increased rapidly in WT and AQP4ex-KO mice, but was delayed in OAP-null mice. AQP4ex-KO mice had the highest water content increase at 20 min. Immunoblot analysis showed stable total AQP4 in WT mice initially, with increases at 30 min. AQP4ex and its phosphorylated form (p-AQP4ex) levels rose quickly, but the p-AQP4ex/AQP4ex ratio dropped at 20 min. AQP4ex-KO mice showed a compensatory rise in canonical AQP4 at 20 min post-AWI. These findings highlight the important role of AQP4ex in water content dynamics in both normal and pathological states. To evaluate brain waste clearance, amyloid-β (Aβ) removal was assessed using a fluorescent Aβ intra-parenchyma injection model. AQP4ex-KO mice demonstrated markedly impaired Aβ clearance, with extended diffusion distances and reduced fluorescence in cervical lymph nodes, indicating inefficient drainage from the brain parenchyma. Mechanistically, the polarization of AQP4 at astrocytic endfeet is essential for efficient clearance flow, aiding interstitial fluid movement into the CSF and lymphatic system. In AQP4ex-KO mice, disrupted polarization forces reliance on slower, passive diffusion for solute clearance, significantly reducing Aβ removal efficiency and altering extracellular space dynamics. Our results underscore the importance of AQP4ex in both brain water homeostasis and solute clearance, particularly Aβ. These findings highlight AQP4ex as a potential therapeutic target

†Pasqua Abbrescia and Gianluca Signorile contributed equally to the work (co-first authors).

*Correspondence:
Antonio Frigeri
antonio.frigeri@uniba.it

Full list of author information is available at the end of the article

for enhancing waste clearance mechanisms in the brain, which could have significant implications for treating brain edema and neurodegenerative diseases like Alzheimer's.

Keywords Aquaporin-4, AQP4ex, Glymphatic system, Brain edema, Amyloid-β clearance, Neurodegenerative diseases

Introduction

The water channel aquaporin-4 (AQP4) plays a pivotal role in regulating water balance within the mammalian brain due to its strategic placement at brain fluid interfaces, such as the end-feet of astrocytic processes facing cerebral capillary [1]. The role of AQP4 in brain edema has been extensively studied and AQP4-null mice provide compelling evidence of AQP4's involvement in maintaining cerebral water balance. AQP4-null mice exhibit protection against cytotoxic brain edema induced by conditions such as water intoxication, brain ischemia, or meningitis [2]. Conversely, AQP4 deletion exacerbates vasogenic brain edema caused by factors like tumors, cortical freezing, intraparenchymal fluid infusion, or brain abscess [3].

The accumulation of fluid in the brain can disrupt normal flow within the network responsible for clearing interstitial waste products, further impeding proper water and metabolite removal. This creates a vicious cycle that exacerbates neuronal damage and edema. Recent findings suggest the existence of a glymphatic system [4], in which AQP4 is essential for accelerating waste clearance, especially during sleep [5]. This opens new possibilities regarding AQP4's involvement in protein accumulation diseases, such as Alzheimer's disease where age-related changes in AQP4 polarization, glymphatic clearance, and amyloid-β (Aβ) deposition appear interconnected. Recent studies have shown an strong reduction in glymphatic function observed in aging brains, along with increased astrocyte reactivity and Aβ accumulation [6]. The inefficient clearance of Aβ is a critical factor in Alzheimer's disease progression, leading to neuroinflammation, disrupted neural communication, and cognitive decline [7].

AQP4 is expressed in two predominant isoforms, M23 and M1, which assemble in the plasma membrane to form highly organized two-dimensional supramolecular structures [8].

known as orthogonal arrays of particles (OAPs), visible through freeze-fracture electron microscopy [9]. Among these isoforms, AQP4-M23 forms OAPs [10, 11], while AQP4-M1 alone lacks this capacity [12], as demonstrated also in transgenic AQP4M23 knockout mice (OAP-null mice) [13]. Moreover, AQP4 mRNA undergoes robust translational readthrough processing to generate two additional extended isoforms M1ex and M23ex [14], which contain a 29-amino-acid C-terminal extension [15]. Studies involving AQP4ex knockout mice (AQP4ex-KO) have demonstrated that these extended isoforms play a crucial role in the assembly and confinement of perivascular OAPs, acting as structural components of the glial endfoot membrane [16, 17].

Recent research has identified a phosphorylated form of AQP4 at Ser335 within the extended sequence (p-AQP4ex), conserved across human, mouse, and rat AQP4ex [18]. p-AQP4ex is strongly expressed in supramolecular assemblies at the perivascular astrocyte endfeet in the human brain. In *vitro* experiments have shown that phosphorylation in the C-terminal extension affects water channel activity, suggesting that this post-translational modification might influence AQP4 activity at the blood-brain barrier (BBB), potentially leading to functional effects under both physiological and pathological conditions [15].

Given the significant presence of AQP4ex in perivascular astrocyte processes, which envelop nearly the entire surface of cerebral blood vessels, it is reasonable to hypothesize that AQP4ex may play a role in the development of edema observed in many pathological conditions [2, 3, 19]. Recent studies have reported that AQP4ex is downregulated in fresh biopsies from glioblastoma patients, and AQP4 delocalization and subsequent reduction are anticipated by AQP4ex alterations from the peritumoral to the tumoral region [20]. Furthermore, BBB alteration and edema index correlated with AQP4ex alteration levels, confirming the role of AQP4ex in vasogenic edema accumulation in the peritumoral area [20].

Recent studies have investigated the involvement of the extended AQP4 isoform in efficient Aβ clearance and identified small molecule compounds suitable for therapeutic intervention [21]. However, the specific roles of AQP4ex in brain physiological homeostasis, edema, and waste clearance remain unclear.

The aim of this study is twofold: first, to evaluate the contributions of the two physiologically predominant AQP4 isoforms—the OAP-forming isoform (M23) and the perivascular localization-controlling isoform (AQP4ex)—in cerebral edema; and second, to investigate the role of AQP4ex in brain waste clearance. Using an acute water intoxication (AWI) model to induce brain swelling without BBB damage, and employing two transgenic mouse models (AQP4ex-KO and OAP-null), we examined the role of AQP4 isoforms and their localization in astrocytic water exchange control under osmotic stress. Additionally, the contribution of AQP4ex to brain waste clearance was assessed using fluorescent Aβ injected into the striatum and evaluating its removal.

Our results highlight the crucial role of AQP4ex in brain water homeostasis and waste clearance, offering new insights into their physiological functions and potential therapeutic targets [22].

Materials and methods

Animals

Experiments were conducted in accordance with the European directive on animal use for research, and the project was approved by the Institutional Committee on Animal Research and Ethics of the University of Bari and the Italian Health Department (Project No. 571/2018-PR, 27th July 2018). Experiments were performed on 3-month-old (adult) mice. AQP4ex knock-out, OAP-null were generated using CRISPR/Cas9-mediated genome engineering and previously described [13, 16]. Mice were maintained under a 12-hour dark/light cycle, with a constant room temperature and humidity (22±2 °C, 75%), and had access to food and water ad libitum. All experiments were designed to minimize the number of animals used and their suffering.

Assessment of blood–brain barrier permeability

To verify BBB integrity, we followed the Evans Blue intracaudal injection protocol described by Alves da Silva et al. [23]. Briefly, Evans blue dye (0.5% in PBS) binds to albumin, a plasma protein. If the BBB is intact, albumin-bound dye cannot cross it and will not be present in the brain parenchyma. A dose of 4 ml/kg of dye was injected into one of the two lateral caudal veins of each mouse. Successful injection was confirmed by the blue coloration of the nose and paws. After 2 h, the animals were perfused with PBS for 15 min to clean the vessels and remove excess dye. Organs of interest were then removed and immediately stored in PBS. The tissue was homogenized, sonicated, and centrifuged for 30 min at 15,000 rcf at 4 °C. The supernatant was collected, mixed with 60% trichloroacetic acid (1:1 ratio) to precipitate proteins, and stored overnight at 4 °C. The solution was centrifuged again for 30 min at 15,000 rcf at 4 °C, and the Evans blue concentration was measured with a spectrophotometer at 610 nm. Concentration values were obtained by interpolating the absorbance readings on a calibration curve with known dye concentrations.

Acute Water Intoxication Model (AWI)

The acute water intoxication model was used to induce acute hyponatremia (HN) [2], which lowers extracellular Na+concentration, creating an osmotic gradient that causes water to move from the bloodstream into the brain parenchyma, leading to astrocyte swelling at the BBB. Mice received an intraperitoneal injection of distilled water equal to 20% of their body weight, along with DDAVP (0.4 µg/kg). Mice were sacrificed by cervical dislocation at baseline and 10, 20, and 30 min after AWI, and their brains were immediately dissected out.

Brain water content evaluation

Brain water content was evaluated using the wet-to-dry technique, widely reported in the literature [3, 24, 25]. After brain collection, the right hemisphere was immediately weighed, then placed in an Eppendorf tube and dehydrated in an oven at 100 °C for 24 h. The dehydrated hemisphere was then weighed, and the water content was calculated using the following equation:

$$water\,content\, = \,(1 - dry\,weight\,/wet\,weight) \times 100\%.$$

Antibodies

For immunoblot experiments, the following primary antibodies were used: rabbit polyclonal anti-AQP4 (1 mg/ml, A5971, Sigma-Aldrich, Saint Louis, MO) diluted 1:8,000; custom rabbit polyclonal anti-mouse AQP4ex (0.972 mg/ml) diluted 1:2,000; custom rabbit polyclonal anti-mouse p-AQP4ex (0.359 mg/ml,) diluted 1:2000. The secondary antibody used was goat anti-rabbit IgG-HRP (Bio-Rad, California, USA), diluted 1:3,000.

Brain protein lysates

After dissection, the left hemisphere of each mouse was dissolved in seven volumes of BN buffer (1% Triton X-100, 12 mM NaCl, 500 mM 6-aminohexanoic acid, 20 mM Bis-Tris, pH 7.0; 2 mM EDTA; 10% glycerol) with a protease inhibitor cocktail (Roche Diagnostic, Monza, Italy). Tissue lysis was performed on ice for 1 h, and the samples were then centrifuged at 17,000 × g for 30 min at 4 °C. Supernatants were collected, and total protein content was calculated using the BCA Protein Assay Kit (Pierce-Thermo Fisher Scientific, USA).

Western blotting

SDS and western blot have been performed as previously described [15, 18]. Briefly, membrane proteins dissolved in Laemmli were resolved on a 13% polyacrylamide gel, and transferred onto PVDF membranes (Immobilon PVDF; Millipore) for immunoblot analysis. After transfer, membranes were blocked and incubated with primary antibodies as described in the "Antibodies" section. After washing, membranes were incubated with peroxidase-conjugated secondary antibodies and washed again. Reactive proteins were revealed with an enhanced chemiluminescent detection system (Clarity Western ECL substrate, Bio-Rad) and visualized on a ChemiDoc Touch imaging system (Bio-Rad). Images were analyzed using Image Lab (Bio-Rad). Red Ponceau staining was used to verify total protein loading across the lanes and to correct (normalize) the protein content in each lane. AQP4,

AQP4ex, and p-AQP4ex expression levels were represented as percentage changes from the baseline level, set at 100% and indicated in the images as red dashed line. The relative percentage of p-AQP4ex was also represented as the proportion of total AQP4ex, indicating the change in the phosphorylated isoform relative to the total extended isoforms.

Intra striatum injection of amyloid-B

Three-month-old AQP4 WT and AQP4ex-KO mice were anesthetized by intraperitoneal injection of a mixture of Ketamine (100 mg/kg) and Xylazine (10 mg/kg) and secured in a stereotaxic apparatus. Mice were injected with 1 µl of amyloid-β (1–42) Hylexa Fluor-488 (200 µg/ml) in the striatum (coordinates: bregma + 1.5 mm, lateral −1.5 mm, depth −2 mm) using a Nanoject II auto nanoliter injection system (Drummond Scientific Company) at a rate of 23 nL/second. Six hours after injection, mice were transcardially perfused with 4% paraformaldehyde in PBS. Brains and ipsilateral deep cervical lymph nodes were immersed in 4% PFA, postfixed overnight, cryoprotected, included in OCT, and stored at -80 °C. Tissues were sliced at 10 µm thickness using a cryostat (CM 1900; Leica, Wetzlar, Germany) at -20 °C and collected on SuperFrost Plus adhesion slides (Thermo Fisher Scientific) with Mowiol (Sigma-Aldrich) and DAPI (Life Technologies). Sections were observed using a LEICA EL6000 microscope with an ACS/APO 10×/0.30 objective.

Semi-quantitative analysis

Deep cervical lymph nodes and brains from AQP4-WT and AQP4ex mice were analyzed. Semiquantitative analysis of fluorescence intensity of amyloid-β (1–42) Hylexa Fluor-488, was carried out from AQP4-WT and AQP4ex mice at the cortical and medullary regions of deep cervical lymph node. Images were captured at 10x magnification using LAS-X software, and mean fluorescence intensity values were collected from four regions of interest (ROIs) for each area. To quantify the spread of the fluorescent signal from the injection site, the space constant λ (µm-1) was calculated. Four linear ROIs were analyzed starting from the injection site towards the brain parenchyma using ImageJ software. Decay curves were generated by averaging fluorescence intensities from these ROIs and normalizing to maximum intensity. Exponential fitting was applied to the curves to visualize fluorescence decay over distance, resulting in interpolated curves for each animal from which the space constant (λ) was derived.

Statistical analysis

Results are reported as mean ± standard error of the independent experiments indicated in figure. Statistical analysis was performed using GraphPad Prism 9 (GraphPad Software, San Diego, CA, USA) by t-test for unpaired data or analysis of variance (ANOVA), followed by Tukey's test. A $^{*}p$-value < 0.05 was considered statistically significant.

Results

BBB Integrity and brain water content in basal condition

Earlier research involving our two transgenic mouse models showed that AQP4ex-KO and OAP-null mice were grossly indistinguishable from wild type littermates [13, 16].

To evaluate the impact of the absence of AQP4ex and M23 isoforms in BBB permeability, the Evans-Blue assay was performed [26]. Data reported in Fig. 1a show very low levels of the dye in the brain of both transgenic animals, similar to wild-type, indicating that the BBB in AQP4ex and OAP-null mice is not substantially altered in mice under basal condition. However, evaluation of brain water content showed that AQP4ex-KO mice had a significantly lower water content compared to WT and to OAP-null mice (Fig. 1b). These data suggest that AQP4ex is critical for maintaining normal brain water content but is not necessary for maintaining BBB integrity under basal conditions.

Brain edema formation

Systemic hyponatremia was reproduced using the widely applied acute water intoxication (AWI) mouse model [2, 27] as a model of cytotoxic brain edema. AWI induces extremely elevated intracranial pressure (ICP) (>40 mmHg) few minutes after water injection which restricts brain perfusion [28] and results in the development of severe cerebral ischemia that determines the mouse death within 60 min [2]. Brain water content was measured at 10, 20 and 30 min of AWI.

Brain water content increased similarly in all genotypes after AWI confirming the model's efficacy in inducing brain water accumulation (Fig. 2a). At 10 min both WT and AQP4ex-KO showed significant water content increases, while OAP-null did not show a statistically significant increase compared to untreated animals. At 20 min, AQP4ex-KO exhibited the highest water content increase compared to WT and OAP-null mice (Fig. 2b, middle). After 30 min water content increase was similar across all genotypes indicating the brains inability to manage water accumulation beyond this threshold, leading to irreversible damage [28].

AQP4 expression in WT mouse brain after acute water intoxication

Immunoblot experiments evaluated AWI effects on AQP4 isoform protein expression in WT mice. Total AQP4 levels remained stable at 10 and 20 min but increased at 30 min (Fig. 3a-b). AQP4ex protein

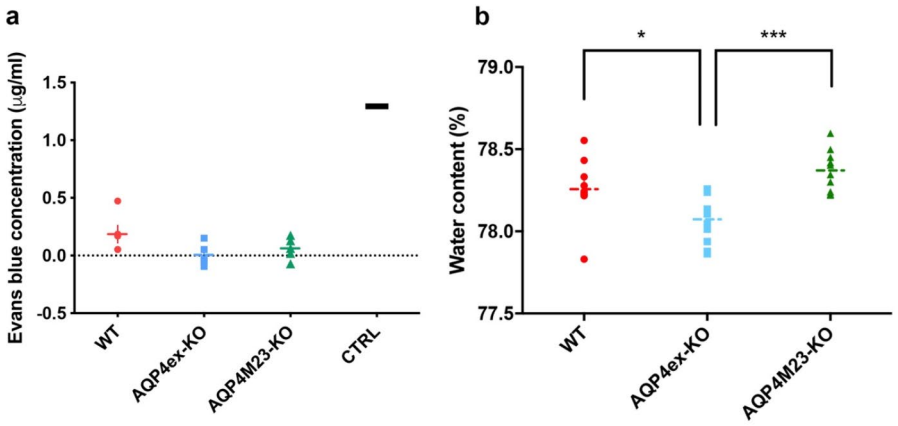

Fig. 1 Characterization of blood vessel permeability and brain basal water content. (**a**) Aligned dot plot showing quantitation of Evans Blue extravasation in WT (red), AQP4ex-KO (blue) and OAP-null (green) mice brain after intracaudal injection of dye. No differences among genotypes are observed ($n = 5$ for each analyzed group). The CTRL value is from a non-perfused animal. (**b**) Basal brain water content expressed in percentage. Aligned dot plot shows significantly reduced brain water content in AQP4ex-KO brain compared to WT and OAP-null. One-way ANOVA, Tukey's multiple comparisons test, $*p < 0.05$, $***p < 0.0001$; data are expressed as means ± SEM

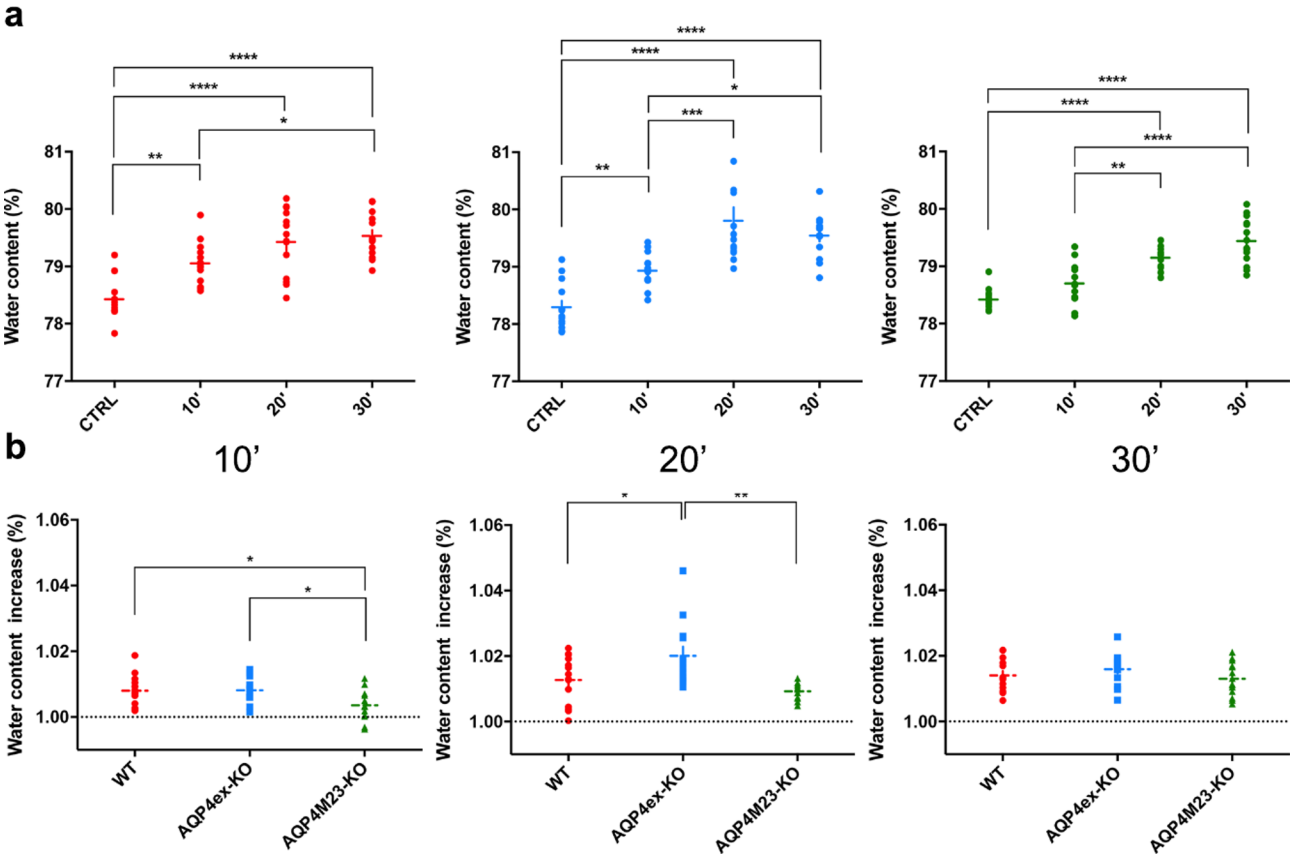

Fig. 2 Evaluation of brain water content after acute water intoxication at different time points. (**a**) Brain water measurements expressed as percentage after 10′, 20′ and 30′ of water intoxication in WT (red), AQP4ex-KO (blue) and OAP-null (green) mice. (**b**) Comparison of brain water content between different genotypes at each time point of AWI. Data were expressed as fold increase compared to basal water content for each genotype, set at 1.00 and indicated as black dashed line. WT and AQP4ex-KO showed higher water increase compared to OAP-null initially, but AQP4ex-KO had greater water accumulation at 20 min. Data are expressed as means ± SEM. ($*p < 0.05$, $**p < 0.01$, $***p < 0.001$, $****p < 0.0001$, One-Way ANOVA with post hoc comparison via a Bonferroni multiple comparison) $n = 14$, except for (**a**) AQP4ex-KO 20′ ($n = 13$), AQP4M23-KO 10′ and 20′ ($n = 12$); (**b**) AQP4M23-KO 10′ ($n = 12$), AQP4ex-KO 20′ ($n = 13$), AQP4M23-KO 20′ ($n = 12$)

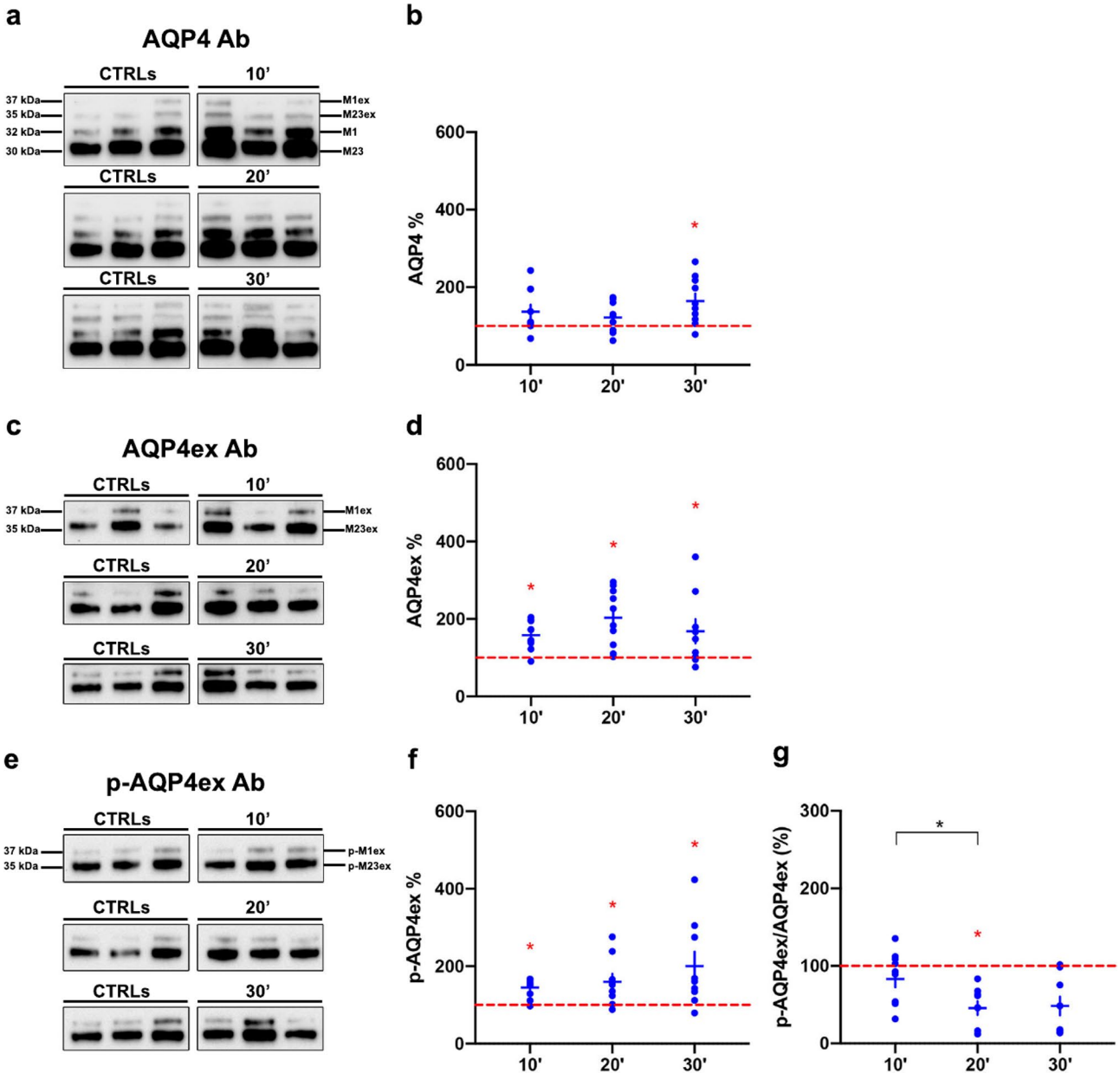

Fig. 3 AQP4 isoforms protein expression in WT mice after different time points of AWI. (**a, c, e**) Immunoblot results of AQP4, AQP4ex and p-AQP4ex expression in three different untreated (CTRLs) and treated mice at 10, 20 and 30 minuses post-AWI. Western blot experiments are representative and the samples shown belong to the same electrophoretic run. (**b, d, f**) Results of the densitometric analysis shown as the percentage variation compared to baseline (red dashed line) of AQP4, AQP4ex and P-AQP4ex respectively (Red asterisk indicates the Student's t-test significant differences for the comparison with basal level, while the black one indicates the comparison between different time points). (**g**) Ratio between p-AQP4ex and AQP4ex showing that only half of additional AQP4ex was phosphorylated at 20 min. Data are expressed as means ± SEM (*$p < 0.05$; One-Way ANOVA $n = 10$)

increased at all time points (Fig. 3c-d), and p-AQP4ex levels similarly increased (Fig. 3e-f). The p-AQP4ex to AQP4ex ratio decreased at 20 min, indicating reduced phosphorylation efficiency (Fig. 3g). This suggests that AQP4ex phosphorylation is crucial for AQP4 function at astrocytic endfeet, probably impacting water dynamics and/or localization. It is rather suggestive that an increase in brain water contents during intoxication triggers time dependent de-phosphorylation processes.

AQP4 expression in AQP4ex-KO mice brain after acute water intoxication

In AQP4ex-KO mice, the absence of AQP4ex led to increased canonical isoforms after 20 min of AWI (Fig. 4a-b). This result parallel the strong water content increase observed after 20 min (Fig. 2) confirming that AQP4ex and the ratio between p-AQP4ex/AQP4ex are involved in the control water increase during AWI.

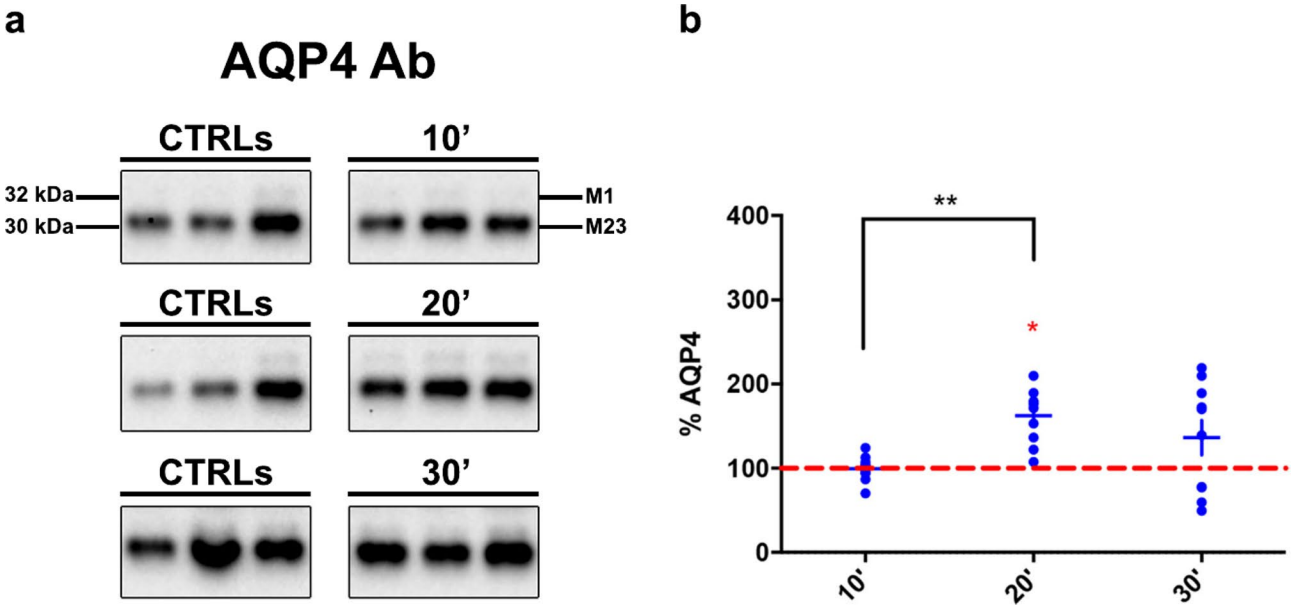

Fig. 4 AQP4 canonical isoform expression in AQP4ex-KO mice post-AWI. (**a**) Typical immunoblot of M1 and M23 isoforms detection in three untreated and treated mice; Western blot experiments are representative and the samples shown belong to the same electrophoretic run. (**b**) Results of the densitometric aanalysis shown as the percentage variation compared to baseline (red dashed line) of AQP4. Note that after 20 min of AWI canonical isoforms significantly increased. (Red asterisk indicates the Student's t-test significant differences for the comparison with basal level, while black one the comparison between different time points, *$p < 0.05$, **$p < 0.01$, $n = 10$)

Impact of AQP4ex on brain parenchymal diffusion and Amyloid-β drainage

Given that basal brain water content was significantly lower in AQP4ex-KO mice we hypothesized that AQP4ex would be also important in regulating the brain parenchyma flow of substances as well as proper brain extracellular environment. To test this hypothesis, we injected fluorescent Aβ (1–42) into the striatum, and fluorescence distribution was measured after 6 h along 50 µm from the injection site (Fig. 5a). This distance was chosen considering that the distances for diffusion of molecules between adjacent brain capillaries are between 20 and 40 µm [29].

Fluorescence evaluation revealed differences in intensity changes between WT and AQP4ex-KO mice (Fig. 5b, c). WT mice showed minimal signal at ~10 µm, while AQP4ex-KO mice showed minimal signal at ~30 µm. The space constant (λ) was strongly reduced in AQP4ex-KO mice, indicating altered intra-parenchymal diffusion of Aβ.

Fluorescence intensity in ipsilateral cervical lymph nodes was lower in AQP4ex-KO mice (Fig. 5b lower and 5d), indicating reduced Aβ drainage. Initial evaluations of the contralateral lymph nodes did not reveal detectable fluorescence signals, and thus, further analysis was not pursued (data not shown). These results suggest that AQP4ex expression controls brain extracellular volume changes and water content (see discussion).

Discussion

In this study we investigated the relevance of AQP4ex in brain water homeostasis and solute clearance. AQP4ex is critical for the proper localization and polarization of AQP4 channels at astrocytic endfeet, Using the water intoxication model and the solute brain injection together with the unique opportunity of the AQP4ex-KO mice, we provide evidence on the crucial role of AQP4ex on brain water balance and amyloid-β (Aβ) clearance. The latter we considered here as a measure of the AQP4ex functional role in the waste clearance system.

Role of AQP4ex in water content dynamics

The regulation of brain water content is fundamental for cerebral homeostasis under both normal and pathological condition. Our data reveals significant differences in basal brain water content between WT and AQP4ex-KO mice with AQP4ex-KO mice exhibiting lower brain water content. This suggests that AQP4ex's critical role in maintaining normal brain water levels.

Following acute water intoxication, brain water content increased in all genotypes, confirming the model's effectiveness in inducing cytotoxic brain edema.

OAP-null mice, in which AQP4 protein is drastically reduced, exhibited a delayed response, in line with a reduced edema formation reported in AQP4-KO mice [2]. AQP4ex-KO mice showed the highest increase in brain water content at 20 min, suggesting AQP4ex's

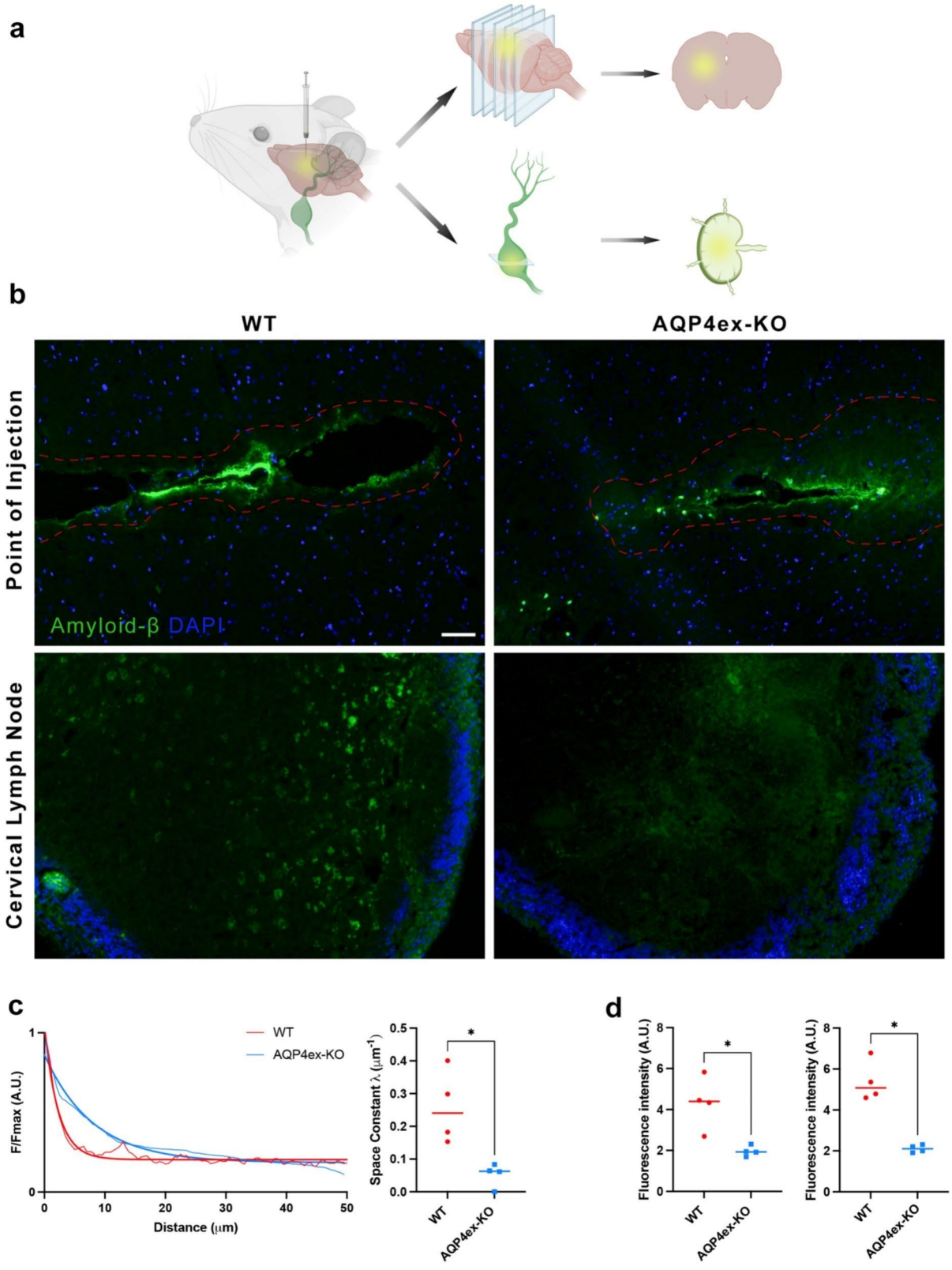

Fig. 5 (See legend on next page.)

(See figure on previous page.)

Fig. 5 Amyloid-β drainage from brain parenchyma. (**a**) Schematic model of the protocol used to evaluate the cleaance of Aβ in the central nervous system of mice. Amyloid-β (1–42) Hylexa Fluor-488 was stereotaxically injected into the striatum and six hours post-injection, the fluorescence of Aβ were assessed after cryosection of brains and lymphnodes. (**b**) Brain section that exhibits the maximum fluorescence intensity among all sections at the injection site was analyzed together with lymph nodes sections. The red dotted line indicates the region where fluorescence levels were detectable. Cell nuclei were stained with DAPI (in blue). Note that the fluorescence intensity of amyloid-β in WT appears lowers than AQP4ex-KO at the point of injection while the ipsilateral cervical lymph nodes have markedly higher levels of fluorescence in WT mice compared to AQP4ex-KO mice. Scale bar 50 µm. (**c**) Aβ fluorescence values plotted as a function of distance from the injection site in the striatum. Quantification of fluorescent signal quantified using the space constant λ (μm^{-1}). (**d**) Quantification of Aβ in cortical (left) and medullar (right) regions of ipsilateral lymph node of WT and AQP4ex-KO mice ($n = 4$). Unpaired t-test, $^{*}p < 0.05$

importance under acute osmotic stress likely through its interactions with other cellular components.

By 30 min post-AWI, brain water content plateaued across all genotypes indicating compromised water regulation beyond this threshold where increased intracranial pressure (ICP) severely restricts cerebral perfusion, leading to irreversible brain damage [30].

These findings highlight the important role of AQP4ex in both normal and pathological states, underscoring its importance in both immediate and sustained responses to brain edema.

Role of AQP4ex protein expression and phosphorylation

Our immunoblot analyses reveal significant insights into the modulation of AQP4ex and p-AQP4ex during AWI. Total AQP4 levels remained relatively stable at early AWI stages but increased significantly at 30 min, indicating a delayed response to prolonged osmotic stress.

Conversely, AQP4ex and p-AQP4ex levels were upregulated at all time points examined, indicating a dynamic and responsive modulation to osmotic stress. The ratio of p-AQP4ex to AQP4ex was similar to control at 10 and 30 min, indicating that the newly produced AQP4ex is phosphorylated at these time points. However, at 20 min, this ratio was significantly reduced. This reduction in phosphorylation at 20 min could be due to several factors, including the presence of regulatory mechanisms that control the timing and extent of phosphorylation, possibly to balance between immediate functional demands and long-term protein stability. Additionally, the phosphorylation process itself may be influenced by the availability of kinases and other modifying enzymes, as well as substrate accessibility.

Interestingly, the time point of 20 min also corresponds to the peak in brain water content observed in AQP4ex-KO mice. The lack of full phosphorylation at this critical time may impair the structural role of AQP4ex in anchoring AQP4 channels at the astrocytic endfeet, thereby affecting the overall water dynamics. This temporal mismatch between AQP4ex production and phosphorylation may result in a transient inability to effectively manage water accumulation, leading to the observed peak in brain water content.

Previous research has demonstrated that phosphorylation of AQP4ex reduces the water permeability of AQP4 channels [15]. However, given that AQP4ex constitutes only a small fraction of the total AQP4 pool, it is unlikely that this phosphorylation plays a significant functional role in water transport. Instead, phosphorylation of AQP4ex likely serves a more structural role, such as anchoring AQP4 at the astrocytic endfeet. This structural role is crucial for maintaining the polarized distribution of AQP4, which is essential for the efficient functioning of the waste clearance system. The enhanced phosphorylation observed at other time points is posited to facilitate interactions with scaffolding proteins and cytoskeletal elements, thereby anchoring AQP4 at the astrocytic endfeet and ensuring efficient water and solute transport.

In AQP4ex-KO mice, the absence of AQP4ex led to a compensatory increase in canonical AQP4 isoforms at 20 min post-AWI. This transient upregulation may reflect an early-stage adaptive mechanism in response to acute osmotic stress, where the brain attempts to compensate for the loss of AQP4ex by increasing the expression of other AQP4 isoforms. However, the brain's inability to sustain this compensation over time may result in the attenuation of this expression by 30 min. The phosphorylation state of AQP4ex may play an essential role in modulating the efficiency of these compensatory mechanisms.

Despite its minor proportion, AQP4ex appears to be essential for maintaining the polarized expression and functionality of AQP4, ensuring efficient water clearance during acute cytotoxic stress. These findings highlight AQP4ex's non-redundant role in regulating brain water homeostasis, particularly in conditions of rapid intracranial pressure changes.

It is reasonable to speculate that the short-term regulation of AQP4ex expression can be influenced by translational mechanisms, especially considering the high levels of AQP4 mRNA [31]. Brain edema can significantly influence these translational mechanisms [32]. The increased osmotic stress and cellular signaling changes associated with brain edema could enhance the efficiency of translational readthrough, leading to an upregulation of AQP4ex production. Factors such as the availability of specific tRNAs, readthrough-promoting sequences in the mRNA, and the presence of translation initiation factors may be modulated under edematous conditions. These modifications may enable the cell to quickly adjust

AQP4ex levels in response to the immediate demands of water homeostasis and edema management.

Role of AQP4ex in solute clearance

Effective clearance of interstitial solutes such as Aβ is critical for preventing neurodegenerative diseases like Alzheimer's. Our data show that AQP4ex is important for this clearance process. In WT mice, the drainage system operates efficiently, as evidenced by the rapid decline in Aβ fluorescence intensity within a short distance from the injection site facilitated by polarized AQP4 at astrocytic endfeet [4]. In contrast, AQP4ex-KO mice exhibited significantly extended Aβ diffusion distances and a larger space constant, indicating impaired clearance due to the loss of AQP4 polarization. The absence of AQP4ex disrupts the structural organization required for effective flow, resulting in a reliance on a slower, less efficient clearance mechanism. This impaired clearance was further validated by reduced Aβ fluorescence in the cervical lymph nodes of AQP4ex-KO mice, indicating compromised drainage from the brain parenchyma. These data are in line with those reported by Sapkota [21].

Recent findings by Mueller et al. [33] suggest that the absence of AQP4ex (AQP4x) may lead to changes in blood-brain barrier (BBB) permeability or impaired efflux mechanisms, though the study could not definitively conclude whether these effects were due to increased leakage or reduced clearance, highlighting the need for further investigation.

In our own study [17] we used high-resolution immunogold cytochemistry to examine the CNS of AQP4ex-KO mice and found no major alterations in key structures, such as capillaries, endothelial cells, or pericytes. This aligns with our current findings, where we observed impaired Aβ clearance without significant changes in BBB permeability. Together, these results suggest that altered clearance mechanisms, rather than direct BBB dysfunction, may be the primary consequence of **AQP4ex** loss. However, we cannot exclude that subtle BBB alterations may also occur in specific brain areas and contribute to the observed defect.

Our data suggest that the impaired clearance in AQP4ex-KO mice aligns more closely with the diffusion model rather than the glymphatic model. The extended diffusion distances and reduced space constants observed indicate that in the absence of AQP4ex, the brain relies more on passive diffusion for solute movement, which is significantly less efficient than the convective flow seen in the glymphatic system of WT mice. This reliance on diffusion results in slower and less effective clearance of Aβ, highlighting the critical role of AQP4ex in maintaining the efficiency of the brain's waste removal system.

An important aspect to consider is the impact of differences in basal water content on solute clearance. AQP4ex-KO mice, which have lower basal brain water content compared to WT mice, may experience altered extracellular space dynamics. Since the BBB is not altered in the AQP4ex-KO mouse, we can conclude that the observed variations are not due to increased vascular permeability. This lower water content could result in a denser extracellular matrix, potentially hindering the movement of solutes such as Aβ. Consequently, the compromised drainage system in AQP4ex-KO mice could be further impaired by the unfavorable conditions for solute diffusion.

The existence and significance of the glymphatic system have been subjects of debate. Proposed in 2017 [6], the glymphatic system describes a waste clearance mechanism dependent on AQP4 polarization at astrocytic endfeet, believed to function predominantly during sleep to facilitate CSF movement through brain parenchyma. However, an alternative diffusion-based theory challenges the robustness of the glymphatic system, suggesting that waste clearance in the brain may not rely heavily on AQP4 channels [34]. Recent research [35] adds to this debate by reporting that brain clearance is reduced during sleep and anesthesia, contrasting with earlier studies. This discrepancy may be due to the mechanisms of waste clearance varying under different physiological states, indicating that the efficiency of waste clearance pathways may be context-dependent and more complex than previously thought.

Our findings contribute to this debate by providing evidence that supports the critical role of AQP4ex in facilitating efficient solute clearance, aligning with the glymphatic model. However, the impaired clearance observed in AQP4ex-KO mice also highlights the complexity of the system and suggests that multiple mechanisms, including passive diffusion, may be involved in brain waste clearance. Further research is necessary to fully understand the mechanisms underlying cerebral waste removal and the potential interplay between different pathways.

Conclusion

In conclusion, AQP4ex plays a crucial role in the polarization of AQP4 channels, which is essential for the efficient functioning of the waste clearance system. This polarization enhances convective flow and solute clearance, preventing the accumulation of neurotoxic substances. The impaired clearance observed in AQP4ex-KO mice reveals the importance of AQP4ex and its phosphorylation in maintaining brain homeostasis. Finally, these mechanisms may provide potential therapeutic targets for enhancing brain waste clearance, potentially mitigating neurodegenerative diseases.

Author contributions
All authors contributed to the study conception and design. PA performed the assessment of blood–brain barrier permeability and the brain water content evaluation after AWI. PA, OV, CP and AC tissue preparation, freezing and analysis. GS intra striatum injection of amyloid-β and semi-quantitative analysis. AF and GPN designed the study. PA and AF wrote the manuscript. All authors read and approved the final manuscript.

Funding
We acknowledge the following co-fundings from Next Generation EU, in the context of the National Recovery and Resilience Plan and funded by the Ministry of University and Research (MUR): project "National Center for Gene Therapy and Drugs Based on RNA Technology", D.D. MUR N. 1035, 17.06.2022, PROJECT CODE CN00000041 - CUP H93C22000430007 to AF and GPN; Investment PE12 project MNESYS: "A Multiscale integrated approach to the study of the nervous system in health and disease" (DM 1553, 11.10.2022) to AF and GPN; Investment PE8 – Project Age-It: "Ageing Well in an Ageing Society" (DM 1557, 11.10.2022) to AF. The views and opinions expressed are only those of the authors and do not necessarily reflect those of the European Union or the European Commission. Neither the European Union nor the European Commission can be held responsible for them. We also acknowledge the project PRIN22 funded by MUR, Code 2022YA9C33 -CUP:H53D2300540006.

Data availability
All data generated or analyzed during this study are included in this published article.

Declarations

Ethics approval and consent to participate
This research was performed in compliance with institutional guidelines and approved by the appropriate institutional committees. All applicable international, national, and/or institutional guidelines for the care and use of animals were followed.

Consent for publication
Not applicable.

Competing interests
The authors declare that they have no competing interests.

Author details
[1]Department of Translational Biomedicine and Neuroscience School of Medicine, University of Bari Aldo Moro, Piazza Giulio Cesare, Bari 70100, Italy
[2]Department of Bioscience, Biotechnology and Environment, University of Bari Aldo Moro, Bari, Italy

Received: 22 July 2024 / Accepted: 26 September 2024
Published online: 10 October 2024

References

1. Verkman AS, Binder DK, Bloch O, Auguste K, Papadopoulos MC (2006) Three distinct roles of Aquaporin-4 in brain function revealed by knockout mice. Biochim Biophys Acta 1758(8):1085–1093. https://doi.org/10.1016/j.bbamem.2006.02.018
2. Manley GT, Fujimura M, Ma T, Noshita N, Filiz F, Bollen AW, Chan P, Verkman AS (2000) Aquaporin-4 deletion in mice reduces Brain Edema after Acute Water Intoxication and ischemic stroke. Nat Med 6(2):159–163. https://doi.org/10.1038/72256
3. Papadopoulos MC, Manley GT, Krishna S, Verkman AS (2004) Aquaporin-4 facilitates reabsorption of excess fluid in Vasogenic Brain Edema. FASEB J 18(11):1291–1293. https://doi.org/10.1096/fj.04-1723fje
4. Iliff JJ, Wang M, Liao Y, Plogg BA, Peng W, Gundersen GA, Benveniste H, Vates GE, Deane R, Goldman SA et al (2012) A paravascular pathway facilitates CSF Flow through the Brain Parenchyma and the Clearance of Interstitial Solutes, including amyloid β. Sci Transl Med 4(147):147ra111. https://doi.org/10.1126/scitranslmed.3003748
5. Hablitz LM, Plá V, Giannetto M, Vinitsky HS, Stæger FF, Metcalfe T, Nguyen R, Benrais A, Nedergaard M (2020) Circadian control of Brain Glymphatic and Lymphatic Fluid Flow. Nat Commun 11(1):4411. https://doi.org/10.1038/s41467-020-18115-2
6. Zeppenfeld DM, Simon M, Haswell JD, D'Abreo D, Murchison C, Quinn JF, Grafe MR, Woltjer RL, Kaye J, Iliff JJ (2017) Association of Perivascular Localization of Aquaporin-4 with cognition and Alzheimer Disease in Aging brains. JAMA Neurol 74(1):91–99. https://doi.org/10.1001/jamaneurol.2016.4370
7. Zuroff L, Daley D, Black KL, Koronyo-Hamaoui M (2017) Clearance of cerebral Aβ in Alzheimer's Disease: reassessing the role of Microglia and Monocytes. Cell Mol Life Sci 74(12):2167–2201. https://doi.org/10.1007/s00018-017-2463-7
8. Nicchia GP, Rossi A, Mola MG, Pisani F, Stigliano C, Basco D, Mastrototaro M, Svelto M, Frigeri A (2010) Higher Order structure of Aquaporin-4. Neuroscience 168(4):903–914. https://doi.org/10.1016/j.neuroscience.2010.02.008
9. Furman CS, Gorelick-Feldman DA, Davidson KGV, Yasumura T, Neely JD, Agre P, Rash JE (2003) Aquaporin-4 square array assembly: opposing actions of M1 and M23 isoforms. Proc Natl Acad Sci U S A 100(23):13609–13614. https://doi.org/10.1073/pnas.2235843100
10. Frigeri A, Gropper MA, Umenishi F, Kawashima M, Brown D, Verkman AS (1995) Localization of MIWC and GLIP Water Channel Homologs in Neuromuscular, epithelial and glandular tissues. J Cell Sci 108(Pt 9):2993–3002. https://doi.org/10.1242/jcs.108.9.2993
11. Verbavatz JM, Ma T, Gobin R, Verkman AS (1997) Absence of orthogonal arrays in kidney, brain and muscle from Transgenic Knockout Mice Lacking Water Channel Aquaporin-4. J Cell Sci 110(Pt 22):2855–2860. https://doi.org/10.1242/jcs.110.22.2855
12. Rash JE, Davidson KGV, Yasumura T, Furman CS (2004) Freeze-fracture and Immunogold Analysis of Aquaporin-4 (AQP4) square arrays, with models of AQP4 Lattice Assembly. Neuroscience 129(4):915–934. https://doi.org/10.1016/j.neuroscience.2004.06.076
13. de Bellis M, Cibelli A, Mola MG, Pisani F, Barile B, Mastrodonato M, Banitalebi S, Amiry-Moghaddam M, Abbrescia P, Frigeri A et al (2021) Orthogonal arrays of Particle Assembly are essential for normal Aquaporin-4 expression level in the brain. Glia 69(2):473–488. https://doi.org/10.1002/glia.23909
14. Loughran G, Chou M-Y, Ivanov IP, Jungreis I, Kellis M, Kiran AM, Baranov PV, Atkins JF (2014) Evidence of efficient stop Codon Readthrough in four mammalian genes. Nucleic Acids Res 42(14):8928–8938. https://doi.org/10.1093/nar/gku608
15. De Bellis M, Pisani F, Mola MG, Rosito S, Simone L, Buccoliero C, Trojano M, Nicchia GP, Svelto M, Frigeri A (2017) Translational Readthrough generates New Astrocyte AQP4 isoforms that modulate supramolecular clustering, Glial Endfeet Localization, and Water Transport. Glia 65(5):790–803. https://doi.org/10.1002/glia.23126
16. Palazzo C, Buccoliero C, Mola MG, Abbrescia P, Nicchia GP, Trojano M, Frigeri A (2019) AQP4ex is crucial for the anchoring of AQP4 at the astrocyte end-feet and for Neuromyelitis Optica antibody binding. Acta Neuropathol Commun 7(1):51. https://doi.org/10.1186/s40478-019-0707-5
17. Palazzo C, Abbrescia P, Valente O, Nicchia GP, Banitalebi S, Amiry-Moghaddam M, Trojano M, Frigeri A (2020) Tissue distribution of the Readthrough Isoform of AQP4 reveals a dual role of AQP4ex Limited to CNS. Int J Mol Sci 21(4):1531. https://doi.org/10.3390/ijms21041531
18. Pati R, Palazzo C, Valente O, Abbrescia P, Messina R, Surdo NC, Lefkimmiatis K, Signorelli F, Nicchia GP, Frigeri A (2022) The Readthrough Isoform AQP4ex is constitutively phosphorylated in the Perivascular Astrocyte Endfeet of Human Brain. Biomolecules 12(5):633. https://doi.org/10.3390/biom12050633
19. Bloch O, Papadopoulos MC, Manley GT, Verkman AS (2005) Aquaporin-4 gene deletion in mice increases focal Edema Associated with Staphylococcal Brain Abscess. J Neurochem 95(1):254–262. https://doi.org/10.1111/j.1471-4159.2005.03362.x
20. Valente O, Messina R, Ingravallo G, Bellitti E, Zimatore DS, de Gennaro L, Abbrescia P, Pati R, Palazzo C, Nicchia GP et al (2022) Alteration of the Translational Readthrough Isoform AQP4ex induces redistribution and downregulation of AQP4 in human glioblastoma. Cell Mol Life Sci 79(3):140. https://doi.org/10.1007/s00018-021-04123-y
21. Sapkota D, Florian C, Doherty BM, White KM, Reardon KM, Ge X, Garbow JR, Yuede CM, Cirrito JR, Dougherty JD (2022) Aqp4 stop Codon Readthrough facilitates Amyloid-β clearance from the brain. Brain 145(9):2982–2990. https://doi.org/10.1093/brain/awac199
22. Frigeri A, Nicchia GP, Svelto M (2007) Aquaporins as targets for Drug Discovery. Curr Pharm Des 13(23):2421–2427. https://doi.org/10.2174/138161207781368738

23. Alves da Silva JA, Oliveira KC, Camillo M (2011) a. P. Gyroxin increases blood-brain barrier permeability to Evans Blue Dye in mice. Toxicon 57(1):162–167. https://doi.org/10.1016/j.toxicon.2010.06.027
24. Migliati ER, Amiry-Moghaddam M, Froehner SC, Adams ME, Ottersen OP, Bhardwaj A (2010) Na(+)-K (+)-2Cl (-) cotransport inhibitor attenuates cerebral Edema following experimental stroke via the Perivascular Pool of Aquaporin-4. Neurocrit Care 13(1):123–131. https://doi.org/10.1007/s12028-010-9376-8
25. Haj-Yasein NN, Vindedal GF, Eilert-Olsen M, Gundersen GA, Skare Ø, Laake P, Klungland A, Thorén AE, Burkhardt JM, Ottersen OP et al (2011) Glial-conditional deletion of Aquaporin-4 (Aqp4) reduces blood-brain water uptake and confers barrier function on Perivascular Astrocyte Endfeet. Proc Natl Acad Sci U S A 108(43):17815–17820. https://doi.org/10.1073/pnas.1110655108
26. Wälchli T, Mateos JM, Weinman O, Babic D, Regli L, Hoerstrup SP, Gerhardt H, Schwab ME, Vogel J (2015) Quantitative Assessment of Angiogenesis, perfused blood vessels and endothelial tip cells in the postnatal mouse brain. Nat Protoc 10(1):53–74. https://doi.org/10.1038/nprot.2015.002
27. Trachtman H, Futterweit S, del Pizzo R (1992) Taurine and osmoregulation. IV. Cerebral taurine transport is increased in rats with hypernatremic dehydration. Pediatr Res 32(1):118–124. https://doi.org/10.1203/00006450-199207000-00023
28. Bordoni L, Li B, Kura S, Boas DA, Sakadžić S, Østergaard L, Frische S, Gutiérrez-Jiménez E (2021) Quantification of Capillary Perfusion in an animal model of Acute Intracranial Hypertension. J Neurotrauma 38(4):446–454. https://doi.org/10.1089/neu.2019.6901
29. Tsai PS, Kaufhold JP, Blinder P, Friedman B, Drew PJ, Karten HJ, Lyden PD, Kleinfeld D (2009) Correlations of neuronal and microvascular densities in murine cortex revealed by direct counting and colocalization of nuclei and vessels. J Neurosci 29(46):14553–14570. https://doi.org/10.1523/JNEUROSCI.3287-09.2009
30. Bordoni L, Jiménez EG, Nielsen S, Østergaard L, Frische SA (2020) New Experimental Mouse Model of Water Intoxication with sustained increased intracranial pressure and mild Hyponatremia without Side effects of Antidiuretics. Exp Anim 69(1):92–103. https://doi.org/10.1538/expanim.19-0040
31. Mayo F, González-Vinceiro L, Hiraldo-González L, Calle-Castillejo C, Morales-Alvarez S, Ramírez-Lorca R, Echevarría M (2023) Aquaporin-4 expression switches from White to Gray Matter regions during postnatal development of the Central Nervous System. Int J Mol Sci 24(3):3048. https://doi.org/10.3390/ijms24033048
32. Papadopoulos MC, Verkman AS (2007) Aquaporin-4 and Brain Edema. Pediatr Nephrol 22(6):778–784. https://doi.org/10.1007/s00467-006-0411-0
33. Mueller SM, McFarland White K, Fass SB, Chen S, Shi Z, Ge X, Engelbach JA, Gaines SH, Bice AR, Vasek MJ et al (2023) Evaluation of gliovascular functions of AQP4 Readthrough isoforms. Front Cell Neurosci 17:1272391. https://doi.org/10.3389/fncel.2023.1272391
34. Smith AJ, Verkman AS (2018) The glymphatic mechanism for Solute Clearance in Alzheimer's Disease: game changer or unproven speculation? FASEB J 32(2):543–551. https://doi.org/10.1096/fj.201700999
35. Miao A, Luo T, Hsieh B, Edge CJ, Gridley M, Wong RTC, Constandinou TG, Wisden W, Franks NP (2024) Brain clearance is reduced during sleep and anesthesia. Nat Neurosci 27(6):1046–1050. https://doi.org/10.1038/s41593-024-01638-y

Publisher's note